

---

# Climate data selection for multi-decadal wind power forecasts

---

**Sofia Morelli \***  
University of Tübingen  
sofia.morelli@uni-tuebingen.de

**Nina Effenberger \***  
Cluster of Excellence Machine Learning  
University of Tübingen  
nina.effenberger@uni-tuebingen.de

**Luca Schmidt \***  
Cluster of Excellence Machine Learning  
University of Tübingen  
luca.schmidt@uni-tuebingen.de

**Nicole Ludwig**  
Cluster of Excellence Machine Learning  
University of Tübingen  
nicole.ludwig@uni-tuebingen.de

## Abstract

Reliable wind speed data is crucial for applications such as estimating local (future) wind power. Global Climate Models (GCMs) and Regional Climate Models (RCMs) provide forecasts over multi-decadal periods. However, their outputs vary substantially, and higher-resolution models come with increased computational demands. In this study, we analyze how the spatial resolution of different GCMs and RCMs affects the reliability of simulated wind speeds and wind power, using ERA5 data as a reference. We present a systematic procedure for model evaluation for wind resource assessment as a downstream task. Our results show that higher-resolution GCMs and RCMs do not necessarily preserve wind speeds more accurately. Instead, the choice of model, both for GCMs and RCMs, is more important than the resolution or GCM boundary conditions. The *IPSL* model preserves the wind speed distribution particularly well in Europe, producing the most accurate wind power forecasts relative to ERA5 data.

## 1 Introduction

Wind is expected to become a dominant source of energy in future power supply [IEA]. For wind to be a reliable source of energy, accurate regional wind forecasts over multi-decadal periods are necessary. Climate model output is a natural choice of data for such analyses, as they provide projections on multi-decadal timescales [e.g. Pryor et al., 2020, Ndiaye et al., 2022]. Climate models are complex physical earth system models whose outputs can differ substantially with large inherent model uncertainties [Zhang and Wang, 2024]. Given this variability, it is crucial to assess the skill of climate models, especially their ability to perform in specific applications of interest such as wind power forecasting [Moemken et al., 2016, Isphording et al., 2024].

Previous research revealed that a higher spatial wind data resolution is more desirable. Not only because it provides more local forecasts Rummukainen [2016], but because the resolution at which a model operates affects which weather phenomena it can resolve [Lucas-Picher et al., 2021]. While higher-resolution models are able to resolve more fine-grained weather phenomena, they come with computational challenges. All models –no matter the spatial resolution– require modeling assumptions and therefore contain errors and uncertainties. It remains unclear which climate data, at which spatial resolution, best represents future wind speeds.

Addressing this question requires a careful evaluation of the different climate model data available. CMIP6 represents the most recent effort to organize and standardize global climate models (GCMs) [Eyring et al., 2016] and making the resulting multi-model output publicly available. Compared to its predecessor CMIP5, CMIP6 offers significant improvements in model performance [Carvalho et al., 2021], particularly regarding surface wind speed simulations [Miao et al., 2023]. A key limitation of GCMs remains their low spatial resolution, typically at  $\geq 100$  km.

---

\*equal contribution

There are techniques to increase the spatial resolution of global climate model output. Regional climate models use GCMs as their input and run at finer resolution [Vautard et al., 2021] to resolve more fine-grained weather phenomena physically. This process, called dynamical downscaling, is, however, computationally intensive. Statistical downscaling methods offer a less resource-demanding alternative, establishing relationships between low-resolution GCM output and localized weather patterns [e.g. Schmidt and Ludwig, 2024]. However, these methods still require high-resolution data to establish such relationship. While RCMs and statistical downscaling techniques can add value in regions with complex terrain or significant land-sea contrasts, they do not always outperform raw GCM data [Rummukainen, 2016]. Furthermore, for CMIP6 there is no unified collection of RCM data available. Given these data limitations, there is a need to investigate whether raw GCM data from CMIP6 can still be valuable for multi-decadal wind power forecasts—despite their lower spatial resolution.

The value of climate models is difficult to assess as climate model outputs are not spatio-temporally aligned. Comparing climate model output to reanalyses such as ERA5 is, therefore, non-trivial. Typically, climate models are validated based on aggregate statistics using their historical runs [e.g. Randall et al., 2007]. In the context of wind power evaluation, an additional challenge arises as the actual variable of interest—wind power—is a derived variable. The variable projected by climate models is wind speed and the relationship between power and speed is complex. To still account for the known non-linearities, other research considers wind speeds cubed [Miao et al., 2023], simulates load factors [MacLeod et al., 2018] or transforms wind speeds to wind power using a turbine power curve [KO et al., 2022].

In the following, we investigate historical wind speeds and derived wind power to analyze how the spatial resolution of global and regional climate model data affects multi-decadal wind power forecasts. In Section 2 we explain how we evaluate different wind (power) projections, in Section 3 we describe our results and in Section 4 we discuss our results as well as shortcomings and future work.

## 2 Methods

To compare the influence of climate model resolution on multi-decadal wind power forecasts, we investigate wind speeds using climate models and subsequent wind power predictions. In the following, we describe the data we use and how we perform evaluations.

### 2.1 Data

In our analysis, we compare the reanalysis dataset ERA5 [Hersbach et al., 2020] to global climate model data from ten CMIP6 models [Eyring et al., 2016] as well as regional climate model data from CORDEX [Giorgi and Gutowski Jr, 2015] based on CMIP5 global boundary models [Taylor et al., 2012]. An overview of all GCMs and RCMs used can be found in Table A.1 and Table A.2, respectively. We use wind velocities  $u$  and  $v$  at six-hourly instantaneous resolution as these were found to be reliable for multi-decadal predictions in Effenberger et al. [2023]) and compute wind speeds  $w$  as

$$w = \sqrt{v^2 + u^2}. \quad (1)$$

Our study region covers all data points in continental Europe within a rectangle with longitudes  $\in (25^\circ, 73^\circ)$  and latitudes  $\in (-30^\circ, 42^\circ)$ . This means we consider gridded data over land, as shown in Figure 1. We focus on historical runs of climate models from 2005 to 2015. We choose the first ensemble member run typically labeled as *r1i1p1f1*. The original wind speeds  $w_{10}$  are available at 10 m above ground<sup>2</sup>. To account for common wind turbine hub heights, we interpolate all wind speeds to 126 m using a wind profile power law following

$$w_{126} = \left(\frac{126}{10}\right)^\alpha \cdot w_{10}, \quad (2)$$

where the coefficient  $\alpha$  is empirically derived to be about  $\frac{1}{7}$  for neutral stability conditions [Peterson and Hennessey Jr, 1978]. Since the regional model runs from CMIP5 are on a curvilinear grid, we re-grid them to a regular Gaussian grid with a matching spatial resolution ( $0.1^\circ$ ) using bilinear interpolation [Schulzweida, 2023].

### 2.2 Evaluation and metrics

The evaluation is performed on two aspects: wind speed and wind power. While wind power is our ultimate variable of interest, the analysis primarily centers around wind speed, the variable provided by the climate models. Wind

<sup>2</sup>For the MPI CMIP5, the only available six-hourly wind speed data at the time of research, provided on the ESGF node [Giorgetta et al., 2012], were at an altitude of 1500 m. Therefore,  $w_{10}$  changes to  $w_{1500}$  in the power law to extrapolate the CMIP5 GCM model data to 126 m.

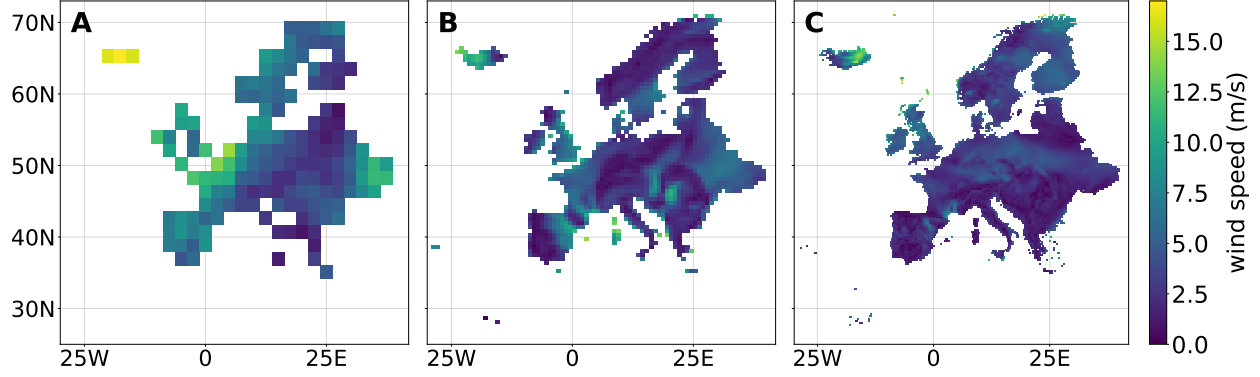


Figure 1: Example of gridded wind speed data over Europe. A single time frame of the same day (01.01.2005) of the lowest resolution CMIP6 data set NCC-LR (A), the highest resolution CMIP6 data set MOHC-HR (B) and the ERA5 reanalysis data set (C).

power can be estimated from wind speed using a theoretical wind power curve. Due to the non-linear nature of this relationship, however, a comprehensive analysis of wind speed distributions is essential for understanding its implications for wind power.

### 2.2.1 Wind speed distributions

Due to the non-linear relationship between wind speed and wind power (compare Figure 2), models must capture the entire wind speed distribution and not only the mean quantities. To analyze these distributions, we investigate kernel density estimations (KDEs) and use quantitative methods to compare wind speed distributions. Since there is no universal metric for comparing distributions, we employ the Jensen-Shannon distance and the Wasserstein-1 distance, each providing a distinct approach to quantifying differences between distributions.

We estimate wind speed probability distributions using KDEs kernel density estimations ()

$$\text{KDE}(w) = \frac{1}{nh} \sum_{i=1}^n K\left(\frac{w - w_i}{h}\right), \quad (3)$$

using Scott's rule Scott [2010] to select a bandwidth  $h$  and the Gaussian kernel  $K(x)$

$$K(x) = \frac{1}{\sqrt{2\pi}} \exp\left(-\frac{1}{2}x^2\right). \quad (4)$$

**Jensen-Shannon distance** We use the Jensen-Shannon (JS) distance to measure how closely a GCM's KDE wind speed distribution aligns with the ERA5 KDE wind speed distribution. This metric is a symmetrical and smooth variant of the Kullback-Leibler (KL) divergence [Endres and Schindelin, 2003], and is defined as

$$\text{JS}(P_{\text{ref}}, P_{\text{pred}}) = \sqrt{\frac{1}{2}\text{KL}(P_{\text{ref}} \parallel M) + \frac{1}{2}\text{KL}(P_{\text{pred}} \parallel M)}, \quad (5)$$

where  $M$  is the mixture distribution

$$M = \frac{1}{2}(P_{\text{ref}} + P_{\text{pred}}), \quad (6)$$

and  $\text{KL}(P_{\text{ref}} \parallel P_{\text{pred}})$  is the KL divergence between the reference distribution  $P_{\text{ref}}$  and the predicted distribution  $P_{\text{pred}}$ , defined as

$$\text{KL}(P_{\text{ref}} \parallel P_{\text{pred}}) = \sum_{x \in \mathcal{X}} (P_{\text{ref}}(x) \log\left(\frac{P_{\text{ref}}(x)}{P_{\text{pred}}(x)}\right)). \quad (7)$$

An advantage of the JS distance is that there are no issues related to undefined or infinite values when comparing distributions with zero wind speeds. Additionally, the JS distance is bounded between  $[0, 1]$  (unlike the Wasserstein-1 distance), offering an intuitive interpretation of the results as a similarity measure.

**Wasserstein-1 distance** As an additional way of comparing the wind speed distributions between the GCMs and ERA5 we use the Wasserstein-1 (W1) distance. The metric is based on the concept of *optimal transport* and differs from JS distance in interpretation and mathematical properties. The W1 distance is defined as

$$W(P_{\text{pred}}, P_{\text{ref}}) = \inf_{\gamma \in \Pi(P_{\text{pred}}, P_{\text{ref}})} \mathbb{E}_{(x,y) \sim \gamma} [\|x - y\|_1], \quad (8)$$

where  $\Pi(P_{\text{pred}}, P_{\text{ref}})$  is the set of couplings, i.e., joint distributions whose marginals are  $P_{\text{pred}}$  and  $P_{\text{ref}}$ . Conceptually, the W1 distance quantifies the expected cost of the optimal transport plan that transforms the distribution  $P_{\text{pred}}$  into  $P_{\text{ref}}$  [Arjovsky et al., 2017].

**Extreme wind speeds** Finally, we shift focus to the highest wind speeds resolved by the model. We expect these extreme values to be linked with spatial resolution, as higher-resolution models may better capture more complex atmospheric processes, potentially leading to a more accurate representation of extreme events. In this context, we consider the average of the 100 highest wind speeds to evaluate model performance. Percentile-based evaluation is avoided, as differences in model resolution would result in varying data points for the same percentile across models.

**Linear regression** The CMIP6 datasets differ in their latitude and longitude coordinates, and we use the number of spatial points within the selected area to measure the grid resolution. To examine trends in distance metrics and maximum wind speeds with increasing spatial resolutions, we perform linear-log regression [Montgomery et al., 2021]. We can then describe the distance of each model to ERA5 as a function of the resolution  $r$

$$w_{max}(r) = \beta_0 + \beta_1 \log(r) + \epsilon \quad (9)$$

where  $\epsilon \sim \mathcal{N}(0, \sigma^2)$  is Gaussian noise and  $\beta_0$  and  $\beta_1$  are computed using the method of least squares.

## 2.2.2 Wind power estimation

So far, we focused on wind speed, as wind directions are a direct output from GCMs. However, wind power is our variable of interest and its estimation involves assumptions and simplifications. While wind speed is a proxy, the ultimate goal is to understand how variations in wind speed distributions impact (multi-decadal) wind power estimation. To compute the wind power generation at each grid point, we input the wind speeds at grid points into a wind turbine power curve [Haas et al., 2024]. In the main part of the paper the chosen wind turbine power curve is the Vestas V126-3.45 turbine, with a hub-height of 126 m, see Figure 2. We provide supporting results for other turbines in the Section A. Finally, we compute the cumulative wind power generation by summing over the power generation of all time steps and grid points. The power predictions from the climate models are normalized by the ERA5 predictions to compare relative cumulative wind power estimates across different models.

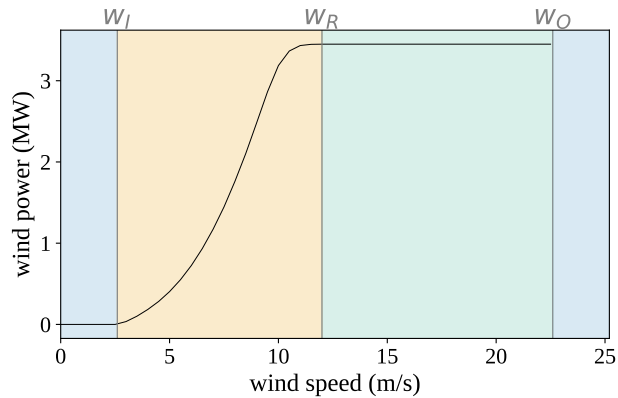


Figure 2: Power curve of the Vestas V126-3.45 turbine. No power is generated for wind speeds below the cut-in wind speed  $w_i$  and above the cut-out wind speed  $w_o$ . Between  $w_i$  and the rated wind speed  $w_r$ , the relationship between speed and power is almost cubic. Between  $w_r$  and  $w_o$  the power output is maximal.

### 3 Results

We investigate the spatial resolution of GCMs and compare wind power predicted by different RCMs. Our results reveal that the choice of the underlying physical model- whether it is an RCM or GCM- is influential, and we do not find systematic trends with increasing resolution.

#### 3.1 Higher resolution of GCM does not imply better forecast

The results in Figure 3 reveal substantial differences in the estimated wind speed KDEs across models. For instance, the JAP model notably deviates from the ERA5 wind speed distribution showing a distinct peak in the lower wind speed range.

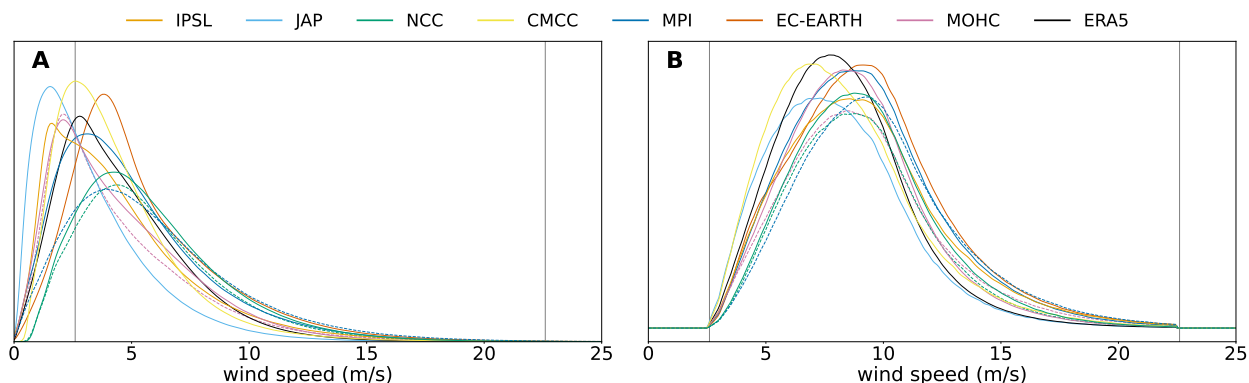


Figure 3: Kernel density estimations of the wind speeds (A) and of the corresponding wind power output (B). When datasets of the same model with different resolutions exist, the low-resolution version is indicated by a dashed line. Horizontal lines indicate the cut-in and cut-out wind speeds of the Vestas V126-3.45 turbine considered in this study. While most wind speeds are  $< 10 \text{ m s}^{-1}$ , most of the wind power is generated by wind speeds  $\sim 10 \text{ m s}^{-1}$ .

We analyze the JS distance and the W1 distance of the GCMs and ERA5 to quantify these distributional differences in wind speeds, as shown in Figure 4. These metrics show substantial variability in each model's ability to capture the wind speed distribution accurately. However, regression analysis shows no statistically significant relationship between the two metrics considered and spatial resolution. This suggests that, although the accuracy of wind speed distributions varies largely between models, this variation is not systematically linked to spatial resolution.

The regression between the average of the 100 highest wind speeds and the logarithm of spatial resolution is significant at the 5% level. This suggests a positive relationship between spatial resolution and the model's ability to represent high wind speeds.

When wind speeds are converted to wind power, accurately capturing specific wind speed quantiles becomes critical. Despite this, the results for cumulative wind power estimated for ten years, shown as a percentage relative to ERA5 power output in Figure 5, reflect similar trends observed in the wind speed distributions. There is considerable variation in the estimated cumulative wind power across different models, with eight models overestimating wind power output relative to ERA5, while two models underestimate it.

Furthermore, relative cumulative power forecasts differ widely, ranging from  $-42.56\%$  to  $68.16\%$  when being compared to ERA5. For example, the GCM IPSL shows the closest alignment with ERA5. When considering the GCMs CMCC and MOHC, the forecasts fall within a range that could be useful for practical applications. This raises the question: given that GCMs can already provide valuable forecasts, is the added complexity and computational cost of regional climate models justified?

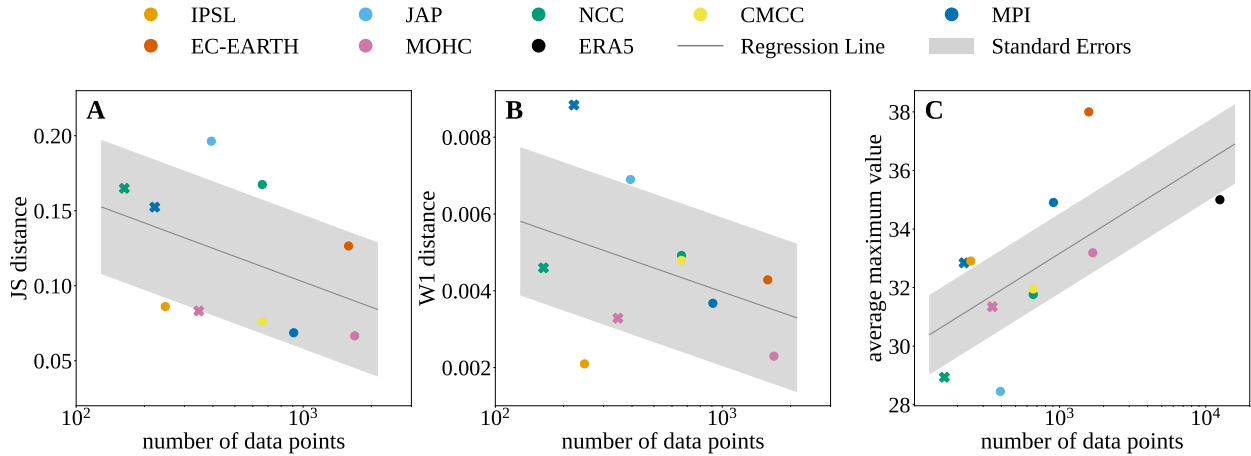


Figure 4: The JS distance (A) and the W1 distance (B) between the wind speeds from CMIP6 and ERA5 and the average over the 100 highest wind speed values (C) are plotted against the spatial resolution (values are given in Table A.3). When datasets of the same model with different resolutions exist, the low-resolution version is indicated by a cross instead of a circle. The gray line represents the log-linear regression fits with standard errors. The regression in (A) and (B) is not statistically significant at a 5% significance level, while the regression in (C) is (see Table A.4).

### 3.2 RCM choice significantly influences the forecast

We further investigate regional model data from CMIP5 and present the corresponding results in Figure 6. For the global model run of the MPI CMIP5 model, we use data extrapolated from a different height (see Section 2). The predictions from CMIP5 overestimate wind power most compared to ERA5. In contrast, all regional model runs and the CMIP6 model run are closer to ERA5. Comparing the spread of the predictions from the MPI model that is downscaled with several regional models (orange in Figure 6) to the prediction of several GCMs downscaled with the regional model SMHI (yellow in Figure 6) reveals that the spread of different regional climate models is bigger than that of one regional model with different boundary conditions. This is also reflected by the variance of the relative power predictions, which is 10.87% for the regional models with the same boundary conditions and 0.26% for the MPI model with different boundary conditions.

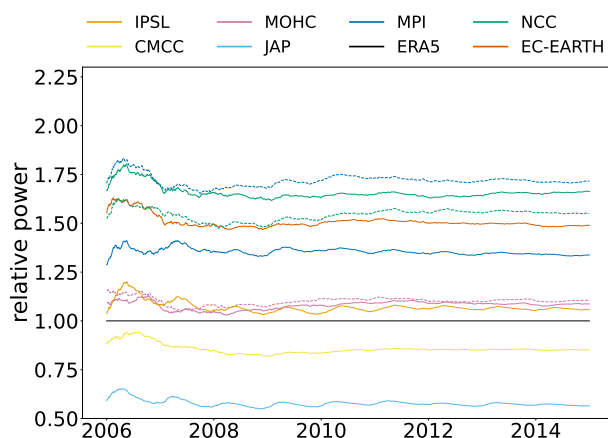


Figure 5: Relative cumulative power of CMIP6 data sets. When datasets with different resolutions run by the same model exist, the low-resolution version is indicated with a dashed line. The choice of GCM has a substantial influence on the power prediction; most GCMs overestimate wind power relative to ERA5.

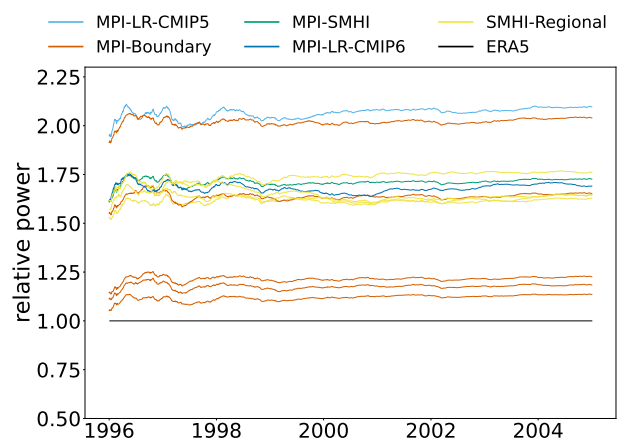


Figure 6: Relative cumulative power of CMIP5 regional and CMIP6 MPI from 1995 to 2005. The spread of the cumulative wind power predictions from multiple RCMs using the output of the MPI model as boundary conditions is larger than the spread using one RCM with different boundary conditions.

## 4 Discussion

We evaluate how GCM’s spatial data resolution affects the reliability of simulated wind speeds for multi-decadal wind power forecasts. Specifically, we focus on ten raw ensemble members of different CMIP6 GCMs over the period 2005 – 2015, comparing wind speed simulations and derived wind power estimates for the European region against ERA5 reanalysis data. Additionally, we investigate whether regional downscaling adds value by comparing the performance of several regional models from CMIP5. We employ various statistical modeling and verification techniques, including directly evaluating wind power to account for the non-linear relationship between wind speed and generated power.

Contrary to the common assumption that a higher resolution provides more reliable wind speeds [Molina et al., 2022, Pryor et al., 2012], we find no clear trend in wind accuracy with increasing spatial resolution. Instead, we observe that the accuracy of wind speed simulations varies substantially across different models. This suggests that the choice of model has a greater impact on wind speed accuracy than spatial resolution itself. Our analysis of regional climate models shows only a small spread in predictions when using different boundary conditions with the same RCM. A much larger spread is visible when comparing different RCMs, further emphasizing the importance of model choice. Therefore, selecting an appropriate climate model should be approached case-by-case, guided by a systematic procedure like the one we present in this paper.

The accuracy of GCMs depends on their ability to capture key climate processes, forcings, and feedback mechanisms [Doblas-Reyes et al., 2021]. Increasing spatial resolution alone does not guarantee an improved representation of these complex processes. This aligns with findings on effective resolution [Klaver et al., 2020], where increases in spatial resolution do not proportionally translate into enhanced representation of meteorological phenomena, as measured by global kinetic energy spectra. Therefore, we advocate for using CMIP6 models for multi-decadal wind power forecasts. Although CMIP6 may have a coarser resolution, it offers notable advancements over its predecessor CMIP5 in simulating climate dynamics and providing more reliable multi-decadal forecasts [Miao et al., 2023]. In line with this rationale, we refrain from applying bias correction or downscaling in our analysis, recognizing that these techniques cannot correct fundamental model misrepresentations and may even disrupt the internal consistency of the climate models [Maraun, 2016, François et al., 2020].

Although our analysis shows no clear trend in wind speed accuracy with increasing spatial resolution, we do find that high-resolution models consistently perform better in capturing the upper tail of the wind speed distribution. This suggests that the benefits of (high-quality) high-resolution models are particularly critical in applications focused on extreme wind events, such as risk assessment.

The IPSL model performs exceptionally well in simulating wind speeds and wind power over Europe, while the MPI-LR model performs the least well. However, our findings are likely region-specific and several limitations must be considered. We simplify our analysis by modeling wind power with a theoretical power curve and interpolating vertically to model wind speeds at a standard hub height. Although ERA5 reanalysis is widely recognized as a reasonable reference [Molina et al., 2021, Olauson, 2018, Kaspar et al., 2020], it still contains notable biases that affect wind power simulations [Staffell and Pfenninger, 2016].

## 5 Conclusion

Climate information is essential for multi-decadal wind power forecasting. Available climate models, among other things, vary substantially in their spatial resolution. We analyze 11 global and regional climate models for their ability to predict long-term wind power.

Our findings highlight the need for high-quality GCMs and RCMs, particularly for wind energy planning. Given the sensitivity of wind power generation to local climate conditions, it is essential that models accurately capture both large-scale dynamics and more local meteorological phenomena. Higher-resolution climate models enhance the representation of extreme wind speeds, yet they do not guarantee improved accuracy in wind speed forecasts. Instead, the selection of the climate models, both GCM and RCM, emerges as a more influential factor for wind speed and power predictions than the spatial resolution itself. As we do not find substantial differences between CMIP5 regional models and CMIP6 global models, we recommend selecting climate models from CMIP6 for multi-decadal wind speed forecasts, as they offer the most current advancements in climate modelling.

## Acknowledgements

This research was funded by the Deutsche Forschungsgemeinschaft (DFG, German Research Foundation) under Germany's Excellence Strategy – EXC number 2064/1 – Project number 390727645, the Tübingen AI Center, and the Athene Grant of the University of Tübingen. The authors thank the International Max Planck Research School for Intelligent Systems (IMPRS-IS) for supporting Nina Effenberger and Luca Schmidt.

## References

- Martin Arjovsky, Soumith Chintala, and Léon Bottou. Wasserstein generative adversarial networks. In *International conference on machine learning*, pages 214–223. PMLR, 2017.
- Mats Bentsen, Dirk Jan Leo Olivieri, Øyvind Seland, Thomas Toniazzo, Ada Gjermundsen, Lise Seland Graff, Jens Bolding Debernard, Alok Kumar Gupta, Yanchun He, Alf Kirkevåg, Jörg Schwinger, et al. NCC NorESM2-MM model output prepared for CMIP6 CMIP historical, 2019. URL <https://doi.org/10.22033/ESGF/CMIP6.8040>.
- Olivier Boucher, Sébastien Denvil, Guillaume Levasseur, Anne Cozic, Arnaud Caubel, Marie-Alice Foujols, Yann Meurdesoif, Patricia Cadule, Marion Devilliers, Josefine Ghattas, et al. IPSL IPSL-CM6A-LR model output prepared for CMIP6 CMIP historical, 2018. URL <https://doi.org/10.22033/ESGF/CMIP6.5195>.
- David Carvalho, Alfredo Rocha, Xurxo Costoya, Maite DeCastro, and Moncho Gómez-Gesteira. Wind energy resource over Europe under CMIP6 future climate projections: What changes from CMIP5 to CMIP6. *Renewable and Sustainable Energy Reviews*, 151:111594, 2021.
- Copernicus Climate Change Service. CORDEX regional climate model data on single levels. <https://cds.climate.copernicus.eu/cdsapp#!/dataset/projections-cmip5-r1i1p1>, 2019. URL <https://cds.climate.copernicus.eu/cdsapp#!/dataset/projections-cmip5-r1i1p1>. Last accessed: 04.09.2024.
- Francisco J Doblado-Reyes, Anna A Sorensson, Mansour Almazroui, Alessandro Dosio, William J Gutowski, Rein Haarsma, R Hamdi, Bruce Hewitson, W-T Kwon, Benjamin L Lamptey, et al. Linking global to regional climate change. 2021.
- EC-Earth. EC-Earth-Consortium EC-Earth3 model output prepared for CMIP6 CMIP historical, 2019. URL <https://doi.org/10.22033/ESGF/CMIP6.4700>.
- Nina Effenberger, Nicole Ludwig, and Rachel H White. Mind the (spectral) gap: how the temporal resolution of wind data affects multi-decadal wind power forecasts. *Environmental Research Letters*, 19(1):014015, 2023.
- Dominik Maria Endres and Johannes E Schindelin. A new metric for probability distributions. *IEEE Transactions on Information theory*, 49(7):1858–1860, 2003.
- Veronika Eyring, Sandrine Bony, Gerald A Meehl, Catherine A Senior, Bjorn Stevens, Ronald J Stouffer, and Karl E Taylor. Overview of the Coupled Model Intercomparison Project Phase 6 (CMIP6) experimental design and organization. *Geoscientific Model Development*, 9(5):1937–1958, 2016.
- Bastien François, Mathieu Vrac, Alex J Cannon, Yoann Robin, and Denis Allard. Multivariate bias corrections of climate simulations: which benefits for which losses? *Earth System Dynamics*, 11(2):537–562, 2020.
- Marco Giorgetta, Johann Jungclaus, Christian Reick, Stephanie Legutke, Victor Brovkin, Traute Crueger, Monika Esch, Kerstin Fieg, Ksenia Glushak, Veronika Gayler, et al. CMIP5 simulations of the max planck institute for meteorology (MPI-M) based on the MPI-ESM-LR model: The historical experiment, served by ESGF, 2012. URL <https://doi.org/10.1594/WDC/CMIP5.MXELhi>.
- Filippo Giorgi and William J Gutowski Jr. Regional dynamical downscaling and the CORDEX initiative. *Annual review of environment and resources*, 40(1):467–490, 2015.
- Sabine Haas, Uwe Krien, Birgit Schachler, Stickler Bot, Velibor Zeli, Florian Maurer, Kumar Shivam, Francesco Witte, Sasan Jacob Rasti, Seth, and Stephen Bosch. wind-python/windpowerlib: Update release, February 2024. URL <https://doi.org/10.5281/zenodo.10685057>.



- H. Hersbach, B. Bell, P. Berrisford, G. Biavati, A. Horányi, J. Muñoz Sabater, J. Nicolas, C. Peubey, R. Radu, I. Rozum, D. Schepers, A. Simmons, C. Soci, D. Dee, and J-N. Thépaut. Era5 hourly data on single levels from 1940 to present. *Copernicus Climate Change Service (C3S) Climate Data Store (CDS)*, 2023. doi: 10.24381/cds.adbb2d47.
- Hans Hersbach, Bill Bell, Paul Berrisford, Shoji Hirahara, András Horányi, Joaquín Muñoz-Sabater, Julien Nicolas, Carole Peubey, Raluca Radu, Dinand Schepers, et al. The ERA5 global reanalysis. *Quarterly Journal of the Royal Meteorological Society*, 146(730):1999–2049, 2020.
- IEA. International energy agency. URL <https://www.iea.org/energy-system/renewables/wind#>. Last accessed: 13.08.2024.
- Rachael N Isphording, Lisa V Alexander, Margot Bador, Donna Green, Jason P Evans, and Scott Wales. A standardized benchmarking framework to assess downscaled precipitation simulations. *Journal of Climate*, 37(4):1089–1110, 2024.
- Johann Jungclaus, Matthias Bittner, Karl-Hermann Wieners, Fabian Wachsmann, Martin Schupfner, Stephanie Legutke, Marco Giorgetta, Christian Reick, Veronika Gayler, Helmuth Haak, et al. MPI-M MPI-ESM1.2-HR model output prepared for CMIP6 CMIP historical, 2019. URL <https://doi.org/10.22033/ESGF/CMIP6.6594>.
- Frank Kaspar, Deborah Niermann, Michael Borsche, Stephanie Fiedler, Jan Keller, Roland Potthast, Thomas Rösch, Thomas Spanghel, and Birger Tinz. Regional atmospheric reanalysis activities at Deutscher Wetterdienst: review of evaluation results and application examples with a focus on renewable energy. *Advances in Science and Research*, 17:115–128, 2020.
- Remko Klaver, Rein Haarsma, Pier L Vidale, and Wilco Hazeleger. Effective resolution in high resolution global atmospheric models for climate studies. *Atmospheric Science Letters*, 21(4):e952, 2020.
- Ogunjobi KO, Ajayi VO, Folorunsho AH, and Ilori OW. Projected changes in wind energy potential using CORDEX ensemble simulation over West Africa. *Meteorology and Atmospheric Physics*, 134(3):48, 2022.
- Tomas Lovato and Daniele Peano. CMCC CMCC-CM2-SR5 model output prepared for CMIP6 CMIP historical, 2020. URL <https://doi.org/10.22033/ESGF/CMIP6.3825>.
- Philippe Lucas-Picher, Daniel Argüeso, Erwan Brisson, Yves Trambly, Peter Berg, Aude Lemonsu, Sven Kotlarski, and Cécile Caillaud. Convection-permitting modeling with regional climate models: latest developments and next steps. *Wiley Interdisciplinary Reviews: Climate Change*, 12(6):e731, 2021.
- Dave MacLeod, Verónica Torralba, Melanie Davis, and Francisco Doblas-Reyes. Transforming climate model output to forecasts of wind power production: how much resolution is enough? *Meteorological Applications*, 25(1):1–10, 2018.
- Douglas Maraun. Bias correcting climate change simulations—a critical review. *Current Climate Change Reports*, 2(4):211–220, 2016.
- Haozeyu Miao, Haiming Xu, Gang Huang, and Kai Yang. Evaluation and future projections of wind energy resources over the Northern Hemisphere in CMIP5 and CMIP6 models. *Renewable Energy*, 211:809–821, 2023.
- Julia Moemken, Mark Reyers, Benjamin Buldmann, and Joaquim G Pinto. Decadal predictability of regional scale wind speed and wind energy potentials over Central Europe. *Tellus A: Dynamic Meteorology and Oceanography*, 68(1):29199, 2016.
- María O Molina, Claudia Gutiérrez, and Enrique Sánchez. Comparison of ERA5 surface wind speed climatologies over Europe with observations from the HadISD dataset. *Int. J. Climatol*, 41(10):4864–4878, 2021.
- María O Molina, João António Martins Careto, Claudia Gutiérrez, Enrique Sánchez, and Pedro M M Soares. The added value of high-resolution EURO-CORDEX simulations to describe daily wind speed over Europe. *International Journal of Climatology*, 43(2):1062–1078, 2022.
- Douglas C Montgomery, Elizabeth A Peck, and G Geoffrey Vining. *Introduction to linear regression analysis*. John Wiley & Sons, 2021.
- Aissatou Ndiaye, Mounkaila Saley Moussa, Cheikh Dione, Windmanagda Sawadogo, Jan Bliefernicht, Laouali Dungal, and Harald Kunstmann. Projected changes in solar PV and wind energy potential over West Africa: an analysis of CORDEX-CORE simulations. *Energies*, 15(24):9602, 2022.

- Jon Olauson. ERA5: The new champion of wind power modelling? *Renewable energy*, 126:322–331, 2018.
- Ernest W Peterson and Joseph P Hennessey Jr. On the use of power laws for estimates of wind power potential. *Journal of Applied Meteorology and Climatology*, 17(3):390–394, 1978.
- Sara C Pryor, Grigory Nikulin, and Colin Jones. Influence of spatial resolution on regional climate model derived wind climates. *Journal of Geophysical Research: Atmospheres*, 117(D3), 2012.
- Sara C Pryor, Rebecca J Barthelmie, Melissa S Bukovsky, L Ruby Leung, and Koichi Sakaguchi. Climate change impacts on wind power generation. *Nature Reviews Earth & Environment*, 1(12):627–643, 2020.
- David A Randall, Richard A Wood, Sandrine Bony, Robert Colman, Thierry Fichet, John Fyfe, Vladimir Kattsov, Andrew Pitman, Jagadish Shukla, Jayaraman Srinivasan, et al. Climate models and their evaluation. In *Climate change 2007: The physical science basis. Contribution of Working Group I to the Fourth Assessment Report of the IPCC (FAR)*, pages 589–662. Cambridge University Press, 2007.
- Jeff Ridley, Matthew Menary, Till Kuhlbrodt, Martin Andrews, and Tim Andrews. MOHC HadGEM3-GC31-MM model output prepared for CMIP6 CMIP historical, 2019a. URL <https://doi.org/10.22033/ESGF/CMIP6.6112>.
- Jeff Ridley, Matthew Menary, Till Kuhlbrodt, Martin Andrews, and Tim Andrews. MOHC HadGEM3-GC31-LL model output prepared for CMIP6 CMIP historical, 2019b. URL <https://doi.org/10.22033/ESGF/CMIP6.6109>.
- Markku Rummukainen. Added value in regional climate modeling. *Wiley Interdisciplinary Reviews: Climate Change*, 7(1):145–159, 2016.
- Luca Schmidt and Nicole Ludwig. Wind power assessment based on super-resolution and downscaling—a comparison of deep learning methods. *arXiv preprint arXiv:2407.08259*, 2024.
- Uwe Schulzweida. CDO user guide, October 2023. URL <https://doi.org/10.5281/zenodo.10020800>.
- David W Scott. Scott’s rule. *Wiley Interdisciplinary Reviews: Computational Statistics*, 2(4):497–502, 2010.
- Øyvind Seland, Mats Bentsen, Dirk Jan Leo Olivie, Thomas Toniazzo, Ada Gjermundsen, Lise Seland Graff, Jens Boldingh Debernard, Alok Kumar Gupta, Yanchun He, Alf Kirkevåg, et al. NCC NorESM2-LM model output prepared for CMIP6 CMIP historical, 2019. URL <https://doi.org/10.22033/ESGF/CMIP6.8036>.
- Iain Staffell and Stefan Pfenninger. Using bias-corrected reanalysis to simulate current and future wind power output. *Energy*, 114:1224–1239, 2016.
- Hiroaki Tatebe and Masahiro Watanabe. MIROC MIROC6 model output prepared for CMIP6 CMIP historical, 2018. URL <https://doi.org/10.22033/ESGF/CMIP6.5603>.
- Karl E. Taylor, Ronald J. Stouffer, and Gerald A. Meehl. An overview of CMIP5 and the experiment design. *Bulletin of the American Meteorological Society*, 93(4):485 – 498, 2012. doi: 10.1175/BAMS-D-11-00094.1. URL <https://journals.ametsoc.org/view/journals/bams/93/4/bams-d-11-00094.1.xml>.
- Robert Vautard, Nikolay Kadyrov, Carley Iles, Fredrik Boberg, Erasmo Buonomo, Katharina Bülow, Erika Coppola, Lola Corre, Erik van Meijgaard, Rita Nogherotto, et al. Evaluation of the large EURO-CORDEX regional climate model ensemble. *Journal of Geophysical Research: Atmospheres*, 126(17):e2019JD032344, 2021.
- Karl-Hermann Wieners, Marco Giorgetta, Johann Jungclaus, Christian Reick, Monika Esch, Matthias Bittner, Stephanie Legutke, Martin Schupfner, Fabian Wachsman, Veronika Gayler, et al. MPI-M MPI-ESM1.2-LR model output prepared for CMIP6 CMIP historical. 2019. doi: 10.22033/ESGF/CMIP6.6595. URL <https://doi.org/10.22033/ESGF/CMIP6.6595>.
- Zhengtai Zhang and Kaicun Wang. Quantify uncertainty in historical simulation and future projection of surface wind speed over global land and ocean. *Environmental Research Letters*, 19(5):054029, 2024.

# Appendices

## Appendix A Supplementary Material

Table A.1: CMIP6 data sets: Labels as used in this paper (first column), names of atmospheric model components (second column), original spatial resolutions in terms of grid specification (third column), number of data points when selecting the land mass of Europe (fourth column), and native resolution (fifth column) as indicated in the references given in the last column.

Label	Model	Grid Resolution	Number of Data Points	Native Resol.	Reference
CMCC	CM2-SR5	$0.9^\circ \times 1.25^\circ$	661	100 km	Lovato and Peano [2020]
EC-EARTH	EC-Earth3.3	T255	1586	100 km	EC-Earth [2019]
IPSL	CM6A-LR	$2.5^\circ \times 1.3^\circ$	247	250 km	Boucher et al. [2018]
JAP	MIROC6	T85	394	250 km	Tatebe and Watanabe [2018]
MOHC-LR	HadGEM3-GC31-LL	N96	347	250 km	Ridley et al. [2019b]
MOHC-HR	HadGEM3-GC31-ML	N216	1688	100 km	Ridley et al. [2019a]
MPI-LR	ESM1.2-LR	T63	222	250 km	Wieners et al. [2019]
MPI-HR	ESM1.2-HR	T127	909	100 km	Jungclaus et al. [2019]
NCC-LR	NorESM2-LM	$2.5^\circ \times 1.875^\circ$	163	250 km	Seland et al. [2019]
NCC-HR	NorESM2-MM	$1.25^\circ \times 0.9375^\circ$	661	100km	Bentsen et al. [2019]
MPI-LR-CMIP5	ECHAM6	T63	222	200 km	Giorgetta et al. [2012]
ERA5	IFS CY41R2	$0.25^\circ \times 0.25^\circ$	12506		Hersbach et al. [2023]

Table A.2: CORDEX data sets: Labels of the global boundary models (first column) and their full model names (second column), labels of the regional models (third column) and their full model names (fourth column). All data sets have resolution  $0.11^\circ \times 0.11^\circ$  12.5km and were withdrawn from Copernicus Climate Change Service [2019].

Label GCM	Model	Label RCM	Model
MPI	MPI-M-MPI-ESM-LR	CNRM	CNRM-ALADIN63
MPI	MPI-M-MPI-ESM-LR	DMI	DMI-HIRHAM5
MPI	MPI-M-MPI-ESM-LR	ETH	CLMcom-ETH-COSMO-crCLIM
MPI	MPI-M-MPI-ESM-LR	ICTP	ICTP-RegCM4-6
MPI	MPI-M-MPI-ESM-LR	MOHC	MOHC-HadREM3-GA7-05
MPI	MPI-M-MPI-ESM-LR	SMHI	SMHI-RCA4
MOHC	MOHC-HadGEM2-ES	SMHI	SMHI-RCA4
NCC	NCC-NorESM1-M	SMHI	SMHI-RCA4
IPSL	IPSL-CM5A-MR	SMHI	SMHI-RCA4
EC-EARTH	ICHEC-EC-EARTH	SMHI	SMHI-RCA4
CNRM	CNRM-CERFACS-CM5	SMHI	SMHI-RCA4

Table A.3: Characteristics of the wind speed samples for all considered models: the mean, the average of 100 highest wind speed values, the Jensen-Shannon (JS), and the Wasserstein-1 (W1) distance to ERA5.

Model	Mean	Max average	JS distance	W1 distance
ERA5	4.58	35.00	-	-
NCC-LR	5.80	28.94	0.165	0.005
NCC-HR	5.84	31.77	0.167	0.005
MPI-LR	5.92	32.84	0.152	0.009
MPI-HR	5.05	34.91	0.069	0.004
MOHC-LR	4.50	31.34	0.083	0.003
MOHC-HR	4.55	33.19	0.067	0.002
JAP	3.37	28.45	0.196	0.007
IPSL	4.56	32.91	0.086	0.002
EC-EARTH	5.54	38.00	0.126	0.004
CMCC	4.32	31.95	0.076	0.005

Table A.4: Regression details for the 100 highest wind speed values, the Jensen-Shannon (JS) and Wasserstein-1 (W1) distance including the regression parameters  $\alpha$  and  $\beta$ , the standard error of the slope, the explained variance ( $100 \cdot R^2$ ) in % and the  $p$ -value of the Overall- $F$ -Test.

	Intercept $\alpha$	Slope $\beta$	Std. Dev.	$R^2$	$p$ -value
JS distance	0.271	-0.056	0.044	16.698	0.241
W1 distance	0.010	-0.002	0.002	12.647	0.313
Max Average	23.807	3.119	1.339	37.626	0.045

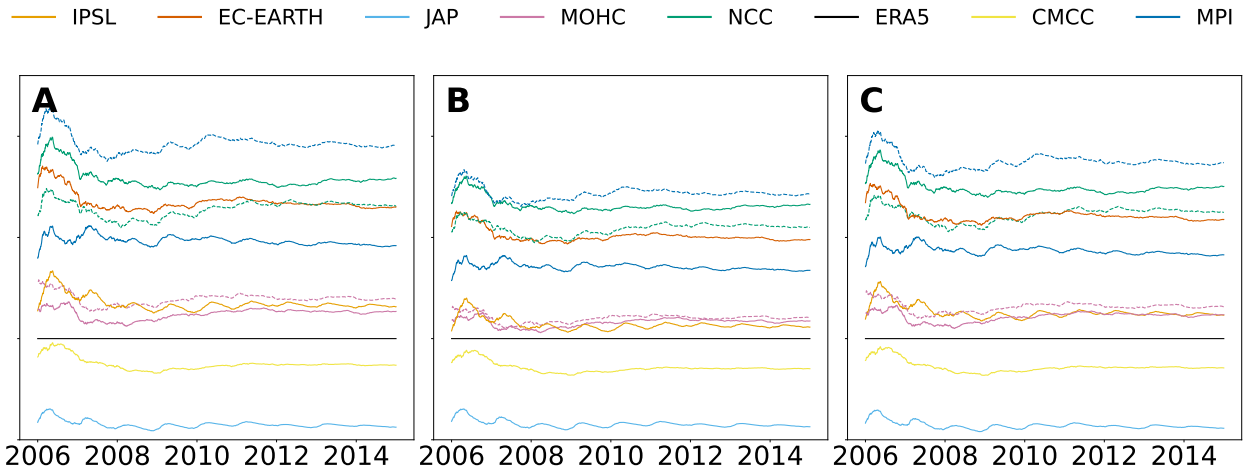


Figure A.1: Relative cumulative wind power for turbine Enercon E-70/2.00 at hub height 85 m (A), turbine Vestas V126-3.45 at hub height 126 m like in the main text (B) and turbine Vestas V164/9.50 at hub height 140 m (C).